CONVECTIVE WAVELENGTH SHIFTS IN THE SPECTRA OF LATE-TYPE STARS

Carlos Allende Prieto, David L. Lambert, Robert G. Tull, and Phillip J. MacQueen

McDonald Observatory and Department of Astronomy
University of Texas
RLM 15.308, Austin, TX 78712-1083,
USA
To appear in ApJL

ABSTRACT

We present ultra-high resolution spectra for a set of nearby F-G-K stars on, or close to, the main sequence. The wavelength shifts of stellar lines relative to their laboratory wavelengths are measured for more than a thousand Fe I lines per star, finding a clear correlation with line depth. The observed patterns are interpreted as convective blue-shifts that become more prominent for weaker lines, which are formed in deeper atmospheric layers. A morphological sequence with spectral type or effective temperature is apparent. Two K giant stars have also been studied. The velocity span between weak and strong lines for these stars is larger than for the dwarfs and subgiants of similar spectral types. Our results show that convective wavelength shifts may seriously compromise the accuracy of absolute spectroscopic radial velocities, but that an empirical correction may be applied to measured velocities.

1. INTRODUCTION

Convection in late-type stars penetrates into the photosphere, producing inhomogeneities. Temperature variations of up to a few hundred Kelvin are apparent in optical images of the Sun, and a velocity field of several kilometers per second is observed in spatially resolved solar spectra. The warmer upflows appear as bright granules surrounded by narrower, cooler downflows. While present technology cannot resolve stellar granulation, there is evidence of its presence in all late-type stars. The temperature and velocity inhomogeneities produce absorption line profiles which are shifted and asymmetric, effects that are readily noticed in ultra-high dispersion stellar spectra.

An extensive literature exists on solar line asymmetries and shifts (see, e.g., Neckel & Labs 1990; Asplund et al. 2000; Pierce & Lopresto 2000). Modern stellar studies were pioneered by Dravins (1974, 1985) and Gray (1980, 1981). Dravins (1999) provides a short review of recent work. Line asymmetries and line shifts are consequences of the same phenomenon and, therefore, give largely equivalent information. When the number of lines measured is limited, but the available features are mostly unblended, line asymmetries carry more information. On the contrary, if the spectrum is heavily crowded, line shifts, which can be measured for many lines, are likely to provide more information. A limited wavelength coverage, largely dictated by the detector size and the scarcity of high-accuracy laboratory wavelengths, steered stellar studies toward the analysis of line asymmetries.

Line bisectors – a measure of the line asymmetry – vary smoothly across the HR diagram (Gray & Toner 1986; Dravins 1987; Gray & Nagel 1989; Dravins & Nordlund 1990). Other parameters, such as rotation, chemical composition, magnetic fields, or binarity, are likely to play a role, but the limited data available have prevented an in-depth study. A recent comprehensive work on the Fe I spectrum (Nave et al. 1994) has provided accurate laboratory wavelengths for 9501 lines. These data and improvements in astronomical instrumentation make it feasible and practical to turn to line shifts as a complement to line bisectors.

Gravitational and convective wavelength shifts systematically affect absolute determinations of radial velocities. Other effects can also introduce systematic radial velocity errors, but they are expected to be less important for most stars (Lindegren, Dravins, & Madsen 1999). Gravitational redshifts are proportional to the mass-to-radius ratio. For spectral lines formed in the photospheres of dwarf stars, the gravitational shift is the same for all lines, in the range between 0.4 and 2 km s^{-1}. When accurate parallaxes and photometry are available, comparison with evolutionary models allows us to determine dwarf masses and radii within 8 % and 6 % , respectively (Allende Prieto & Lambert 1999). It is therefore possible to estimate the gravitational shift within 10 %, yielding worst-case uncertainties of ~ 0.2 km s^{-1}. Convective line shifts may vary with spectral type. The velocity difference between weak and strong lines is about ~ 0.6 km s^{-1} for the Sun (Allende Prieto & García López 1998) and probably more than 1 km s^{-1} for the F5 subgiant α CMi (Procyon; Allende Prieto et al. 2002), but no systematic study across the HR diagram has been published. Obviously, accurate spectroscopic studies of absolute radial velocities cannot afford to neglect these shifts.

In this paper, we analyze optical spectra of several late-type stars obtained with the High Resolution Spectrograph (HRS) coupled to the Hobby-Eberly Telescope (HET). The high quality and large spectral coverage of the spectra allow us to measure line shifts for a large number of Fe I lines. Section 2 describes the observations and the data. In Section 3 we describe the analysis, and in §4 we discuss the results.

2. OBSERVATIONS

Our observations were obtained with the 9.2m HET at McDonald Observatory and the HRS (Tull 1998). The HRS saw first light on March 17, 2001, starting science observations shortly afterwards. This fiber-coupled echelle spectrograph uses an R-4 echelle, cross-dispersing gratings,

and a mosaic of two 2k×4k CCDs. In the selected mode, HRS provides a FWHM resolving power $R \simeq 120,000$ and complete spectral coverage between 4094 and 7890 Å, with the exception of the gap (5977–5999 Å) between the CCDs. The observations were performed in *queue* mode in May and June 2001 (see Table 1). An observation consisted of two exposures that were extracted and combined. The final signal-to-noise (S/N) per pixel was ≥ 400 at most wavelengths.

The spectra were processed with the tasks in the IRAF *echelle* package. We removed the bias signal, flatfielded and extracted the spectra, subtracting the low background in the wide interorder regions. In addition to the program stars observed with the HET, we have included in this study the spectra of the Sun (Kurucz et al. 1984) and α CMi (Allende Prieto et al. 2002).

3. ANALYSIS

3.1. *Stellar parameters*

The effective temperature ($T_{\rm eff}$) has been estimated for all the program stars by one or more authors using the Infrared Flux Method (Blackwell & Lynas-Gray 1994; Alonso et al. 1996, 1999). The $T_{\rm eff}$ of α Boo (Arcturus) has been independently derived by di Benedetto (1998) and Griffin & Lynas-Gray (1999). We have adopted the values in Table 1. All our stars were analyzed by Allende Prieto & Lambert (1999), and we accepted the surface gravities derived there from the $(B-V)$ colors and the *Hipparcos* trigonometric parallaxes. The iron abundances in Table 1 are a straight average of previous spectroscopic analyses compiled by Cayrel de Strobel et al. (2001). A recent discussion of the preferred stellar parameters of α CMi can be found in Allende Prieto et al. (2002). Fe I lines at 4602.00 and 4602.94 Å with accurate gf-values and damping parameters were analyzed with synthetic spectra computed from flux-constant LTE model atmospheres to estimate the projected rotational velocities in Table 1.

3.2. *Measuring the line centers*

A variety of procedures have been used previously to determine the central wavelength of a spectral line. The most popular methods involve some type of least-squares polynomial fitting or polynomial interpolation (see, e.g., Neckel & Labs 1990; Allende Prieto & García López 1998). As the stellar spectral lines are asymmetric, the details of the measuring procedure affect the derived central wavelength. Polynomial least-squares fits are well-suited for error estimation, however, there is some arbitrariness in the selection of the ideal order and wavelength interval to use in the fits. For the slowly rotating stars analyzed here, we have found that a reasonable choice, the same for the whole sample, provides stable results regardless of the exact selection for the order and wavelength interval. Our particular choice is to fit 35 mÅ around the line center with a third order polynomial. Preceding the fitting by a cubic-spline interpolation with a step of 5 mÅ proved useful for the HRS spectra, but degraded slightly the quality of the results for the superior solar atlas.

To estimate the error in a derived central wavelength, we determine the horizontal scatter between the polynomial fit F(λ) and the observed spectrum $f(\lambda)$. For each observed wavelength λ_i considered in the fit, we find numerically the roots of the polynomial $F(\lambda) - f(\lambda_i)$ using Laguerre's method, select the appropriate root, and then derive the rms scatter between the observed and fit wavelengths. Assuming the errors are Gaussian, this scatter is divided by the square root of the number of points entering the polynomial fit to derive the uncertainty $\sigma_{\rm s}$. As an example, application to the solar flux spectrum provides a nearly normal distribution of uncertainties that peaks at 0.00025 Å and shows bumps on the long-value tail, signaling blends. Nave et al. (1994) classify their wavelengths into four categories, depending on their uncertainty ($\sigma_{\rm l}$), which ranges from 0.4 mÅ to more than 10 mÅ. Most lines have errors below 5 mÅ and about half of the lines have errors below 1 mÅ[1].

The uncertainties in the measured wavelength shifts, $\sigma = \sqrt{\sigma_{\rm s}^2 + \sigma_{\rm l}^2}$, are then converted to velocity, and their distribution $n(\sigma)$ is determined. Then, we use $n(\sigma)$ to predict the distribution of errors (δ) in the observed velocity shifts as

$$N(\delta) = \frac{1}{C} \int_0^\infty \frac{n(\sigma)}{\sigma} \exp\left(-\frac{\delta^2}{2\sigma^2}\right) d\sigma, \qquad (1)$$

where C is chosen such that $\int_{-\infty}^{\infty} N(\delta) d\delta = 1$. The derived $N(\delta)$ can be compared to the observations in order to constrain the intrinsic scatter. In all cases, the derived and measured histograms are similar.

3.3. *Searching for correlations*

The number of iron lines identified and measured for each star varies from 1340 to 1569[2]. Solar analyses have shown clear correlations of the line shifts with line strength (Allende Prieto & García López 1998) and wavelength (Hamilton & Lester 1999). We explore here the variation of the shifts with line strength, as this is the dominant effect. The line equivalent width and the central line depth have been the most widely used line strength indicators. As pointed out by Pierce & Lopresto (2000), the use of the equivalent width avoids saturation for the strongest lines. On the other hand, equivalent width measurements are distorted by blends in the line wings which may hardly affect line depths. Blends are a particularly serious problem when dealing with cool stars, as some of those in our sample. Therefore, we have adopted the line depth.

The left-hand panels in Fig. 1 show the line velocity shifts for the stars in our sample as a function of the residual flux at the center of the line $f_{\rm c}$ ($= 1-$ line depth). In these panels, the shifts of the individual lines are marked with dots. Grouping the lines in bins of 0.1 in depth, and after applying a median filter, we derive the average values shown as asterisks with error bars. The solid lines are 3th-order polynomial fits to guide the eye, and the broken lines trace the original median values. We have not attempted to disentangle the stellar radial velocities from the gravitational shifts and the atmospheric motions. The absolute values on the vertical axis have been shifted to

---

[1] This comparison indicates that an extension and improvement of the laboratory wavelengths for neutral iron and other species is desirable. A spectrograph used to obtain stellar spectra may be well suited for this purpose (see Allende Prieto 2001)

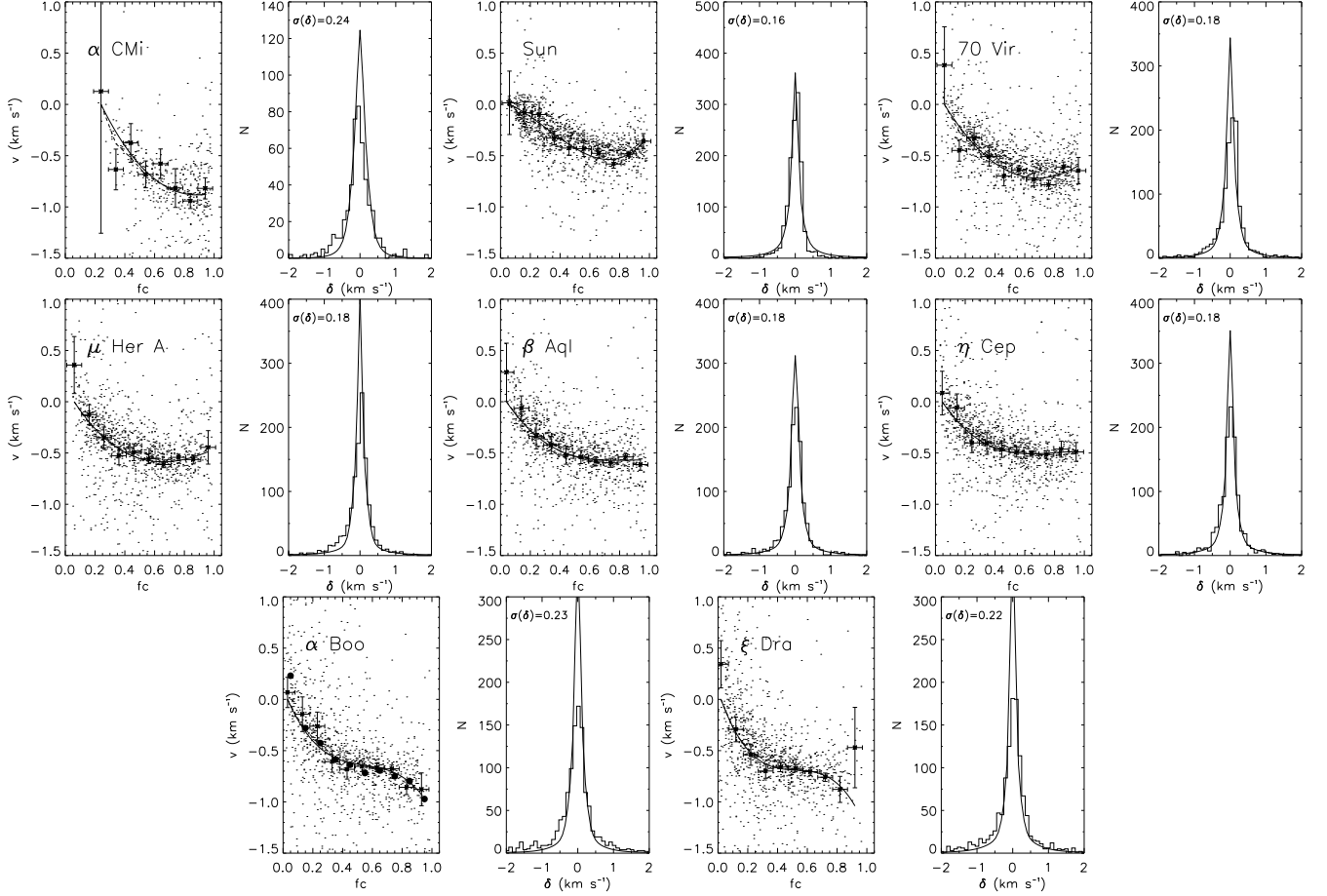[2] With the exception of α CMi, for which only 588 lines were measured

FIG. 1.— The left-hand panels show the relative velocity shifts of Fe I lines with respect to their rest wavelengths. The velocity scale for each star is shifted to have a null velocity for the median shift of the strongest lines considered. The dots show the shifts for the individual lines. The asterisks with error bars are mean values after applying a median filter, and the solid line is a polynomial fit to them. The dashed curve shows the median shifts for the different bins. The right-hand panels show histograms of the scatter of the velocity shifts around the polynomial fit. The expected scatter (see text) is shown by the symmetric solid curve. The mean velocity shifts determined from the analysis of the α Boo atlas of Hinkle et al. (2000) are displayed as filled circles in the left-hand panel for this star.

TABLE 1
OBSERVED SAMPLE

Star	Obs. date	Sp. Type	$T_{\rm eff}$[a] (K)	$\log g$ (dex)	[Fe/H] (dex)	$v \sin i$ (km s^{-1})	$S(v)$ (km s^{-1})
α CMi	McDonald atlas	F5 IV	6530	3.96 (0.02)	-0.05 (0.03)	2.8 (0.1)	0.88
Sun	FTS atlas	G2 V	5770	4.44 (0.01)	0.00	1.9 (0.1)	0.54
70 Vir	June 5	G4 V	5455	4.04 (0.11)	-0.11[b]	3.2 (0.1)	0.72
μ Her A	May 28	G5 IV	5523	3.87 (0.04)	0.23 (0.07)	4.1 (0.2)	0.59
β Aql	June 11	G8 IV	5040	3.56 (0.07)	-0.02 (0.10)	3.1 (0.3)	0.57
η Cep	May 29	K0 IV	4944	3.40 (0.18)	-0.12 (0.14)	3.1 (0.1)	0.51
α Boo	June 9	K1.5 III	4290	2.00 (0.56)	-0.51 (0.03)	3.0 (0.5)	0.93
ξ Dra	May 29	K2 III	4430	2.31 (0.32)	-0.13 (0.04)	5.1 (0.5)	1.04

[a]Uncertainties in $T_{\rm eff}$ are 100 K or smaller

[b]A single measurement is available

have a null median velocity shift for the strongest lines; a condition that the polynomial fits were as well forced to satisfy. The right-hand panels show the scatter of the line shifts about the average points. The scatter expected from Eq. (1), mainly the result of the uncertainties in the laboratory wavelengths, the finite width of the lines, and the presence of photometric noise, is also displayed (thick symmetric curve). The $\sigma(\delta)$ given in the right-hand panels corresponds to a Gaussian fit by least-squares to the observed scatter. The velocity span of the polynomial fits, $S(v)$, is listed in Table 1.

A spectroscopic atlas of α Boo at a superior resolving power and S/N was published by Hinkle et al. (2000). The corresponding left-hand panel in Figure 1 compares the average shifts from our measurements from the atlas (filled circles) with those from the HRS spectrum (asterisks with error bars). The agreement is quite satisfactory. The σ of the scatter in our spectrum and in the atlas agree within 10 m s^{-1}.

4. DISCUSSION

The pattern of the velocity shifts is similar for all the stars, and in qualitative agreement with solar results. The net convective blue shifts of the lines strengthen toward deeper photospheric layers, and therefore affect the weak lines more than the strong ones. Despite our limited sample, there is an indication of a smooth dependence of the average velocity shifts with spectral type. This effect is clearer in our analysis of line shifts than in previous studies using bisectors. As argued in the introduction, this is likely the result of line shifts measurements being less affected by blending than line bisectors in late-G and K type stars.

Our preliminary results indicate that the trend of line shifts as a function of line strength can be determined as a function of spectral type and gravity. At least for late-type dwarfs, assuming the strongest lines in the spectrum are free from convective shifts (as is the case for the solar photosphere), it is possible to correct for convective wavelength shifts to within $\simeq 0.2$ km s^{-1}.

The measured range of wavelength shifts for neutral iron lines is larger in α CMi than in cooler stars of classes IV and V. The range of wavelength shifts is also larger, reaching up to ~ 1 km s^{-1}, for the K giants than for the G-K

dwarfs and subgiants in our sample, which is not surprising. Although their lower effective temperatures provide less flux to transport, their lower atmospheric pressure implies larger convective velocities. Fig. 1 suggests that, once we account for the observational errors, there is little room for intrinsic line-to-line scatter in the F-G-K stars sampled here. Convection is supposed to cease in main sequence stars with spectral types earlier than about F2, but other velocity fields must be present in those atmospheres, judging from the asymmetry of the spectral lines (e.g. Gray & Nagel 1989). Determining accurate absolute radial velocities demands an understanding of the wavelength shifts in the spectra of these stars too.

Solar observations have shown differences in the center-to-limb variation of the granulation along the central meridian and the equator (e.g. Beckers & Taylor 1980; Rodríguez Hidalgo, Collados, & Vázquez 1992). Observations of a large number of stars may then show peculiarities at a given spectral type depending on the orientation of the rotational axis. Stars with enhanced magnetic fields are also expected to be peculiar in terms of observed wavelength shifts, as the enhanced magnetic fields may hinder the convective motions. Furthermore, line shifts may vary with time for stars exhibiting an analog of the solar 11 year cycle.

Observations of line shifts for a significant number of stars with high quality are required for a deeper understanding of granulation in stellar atmospheres, its relationship with other stellar phenomena, and the role of surface convection in the structure and evolution of stars. Our first results show that measurements of convective line shifts are a must in order to derive accurate absolute radial velocities.

REFERENCES

Allende Prieto, C. 2001, The Spectrum of the Th-Ar Hollow-Cathode Lamp Used with the 2dcoudé Spectrograph, http://hebe.as.utexas.edu/2dcoude/thar/ (astro-ph/0111172)
Allende Prieto, C., Asplund, M., García López, R. J., & Lambert, D. L. 2002, ApJ, in press (astro-ph/011055)
Allende Prieto, C., & García López, R. J. 1998, A&AS, 129, 41
Allende Prieto, C., & Lambert, D. L. 1999, A&A, 352, 555
Alonso, A., Arribas, S., & Martínez-Roger, C. 1996, A&A, 313, 873
Alonso, A., Arribas, S., & Martínez-Roger, C. 1999, A&AS, 140, 261
Asplund, M., Nordlund, Å., Trampedach, R., Allende Prieto, C., & Stein, R. F. 2000, A&A, 359, 729
Beckers, J. M., & Taylor, W. R. 1980, Sol. Phys., 68, 41
Blackwell, D. E., & Lynas-Gray, A. E. 1994, A&A, 282, 899
Cayrel de Strobel, G., Soubiran, C., & Ralite, N. 2001, A&A, 373, 159
di Benedetto, G. P. 1998, A&A, 339, 858
Dravins, D. 1974, A&A, 36, 143
Dravins, D. 1985, IAU Colloq. 88: Stellar Radial Velocities, 311
Dravins, D. 1987, A&A, 172, 211
Dravins, D. 1999, ASP Conf. Ser. 185: IAU Colloq. 170: Precise Stellar Radial Velocities, 268

Dravins, D., & Nordlund, Å. 1990, A&A, 228, 203
Gray, D. F. 1980, ApJ, 235, 508
Gray, D. F. 1981, ApJ, 251, 583
Gray, D. F., & Nagel, T. 1989, ApJ, 341, 421
Gray, D. F., & Toner, C. G. 1986, PASP, 98, 499
Griffin, R. E. M., & Lynas-Gray, A. E. 1999, AJ, 117, 2998
Hamilton, D., & Lester, J. B. 1999, PASP, 111, 1132
Hinkle, K., Wallace, L., Valenti, J., & Harmer, D. 2000, Visible and Near Infrared Atlas of the Arcturus Spectrum 3727-9300 Å (San Francisco: ASP)
Kurucz, R. L., Furenlid, I., & Brault, J. 1984, National Solar Observatory Atlas (Sunspot, New Mexico: NSO)
Lindegren, L., Dravins, D., & Madsen, S. 1999, ASP Conf. Ser. 185: IAU Colloq. 170: Precise Stellar Radial Velocities, 73
Nave, G., Johansson, S., Learner, R. C. M., Thorne, A. P., & Brault, J. W. 1994, ApJS, 94, 221
Neckel, H., & Labs, D. 1990, Sol. Phys., 126, 207
Pierce, A. K., & Lopresto, J. C. 2000, Sol. Phys., 196, 41
Rodríguez Hidalgo, I., Collados, M., & Vázquez, M. 1992, A&A, 264, 661
Tull, R. G. 1998, Proc. SPIE, 3355, 387